

Probing decisive answers to dark energy questions from cosmic complementarity and lensing tomography

Mustapha Ishak

Department of Astrophysical Sciences, Princeton University, Princeton, NJ 08544, USA
mishak@princeton.edu

11 November 2018

ABSTRACT

We study future constraints on dark energy parameters determined from several combinations of cosmic microwave background experiments, supernova data, and cosmic shear surveys with and without tomography. In this analysis, we look in particular for combinations of experiments that will bring the uncertainties to a level of precision tight enough (a few percent) to answer decisively some of the dark energy questions. In view of the parameterization dependence problems, we probe the dark energy using two variants of its equation of state $w(z)$, and its energy density $\rho_{de}(z)$. For the latter, we model $\rho_{de}(z)$ as a continuous function interpolated using dimensionless parameters $\mathcal{E}_i(z_i) \equiv \rho_{de}(z_i)/\rho_{de}(0)$. We consider a large set of 13 cosmological and systematic parameters, and assume reasonable priors on the lensing and supernova systematics. For CMB, we consider future constraints from 8 years of data from WMAP, one year of data from Planck, and one year of data from the Atacama Cosmology Telescope (ACT). We use two sets of 2000 supernovae with $z_{max} = 0.8$ and 1.5 respectively, and consider various cosmic shear reference surveys: a wide ground-based like survey, covering 70% of the sky, and with successively 2 and 5 tomographic bins; a deep space-based like survey with 10 tomographic bins and various sky coverages. The one sigma constraints found are $\{\sigma(w_0) = 0.086, \sigma(w_1) = 0.069\}$, $\{\sigma(w_0) = 0.088, \sigma(w_a) = 0.11\}$, and $\{\sigma(\mathcal{E}_1) = 0.029, \sigma(\mathcal{E}_2) = 0.065\}$ from Planck, supernovae and the ground-based like lensing survey with 2 bins. When 5 bins are used within the same combination the constraints reduce to $\{\sigma(w_0) = 0.04, \sigma(w_1) = 0.034\}$, $\{\sigma(w_0) = 0.041, \sigma(w_a) = 0.056\}$, and $\{\sigma(\mathcal{E}_1) = 0.012, \sigma(\mathcal{E}_2) = 0.049\}$. Finally, when the deep lensing survey with 10% coverage of the sky and 10 tomographic bins is used along with Planck and the deep supernovae survey, the constraints reduce to $\{\sigma(w_0) = 0.032, \sigma(w_1) = 0.027\}$, $\{\sigma(w_0) = 0.033, \sigma(w_a) = 0.04\}$, and $\{\sigma(\mathcal{E}_1) = 0.01, \sigma(\mathcal{E}_2) = 0.04\}$. Other coverages of the sky and other combinations of experiments are explored as well. Although some worries remain about other systematics, our study shows that after the combination of the three probes, lensing tomography with many redshift bins and large coverages of the sky has the potential to add key improvements to the dark energy parameter constraints. However, the requirement for very ambitious and sophisticated surveys in order to achieve some of these constraints or to improve them suggests the need for new tests to probe the nature of dark energy in addition to constraining its equation of state.

Key words: cosmology: theory – dark energy – gravitational lensing – large-scale structure of universe

1 INTRODUCTION

One of the most important and challenging questions in cosmology and particle physics is to understand the nature of the dark energy that is driving the observed cosmic acceleration, see e.g. (Weinberg (1989); Carroll et al. (1992); Turner (2000); Sahni & Starobinsky (2000); Padmanabhan (2003); Ishak (2005)). An important approach to this problem is to constrain

the properties of dark energy using cosmological probes. This would provide measurements that would allow one to test various competing models of dark energy. However, due to a high degeneracy within a narrow range of the parameter space, constraining conclusively dynamical dark energy models is going to be a difficult goal to achieve, and much effort and strategy will be needed. Ultimately, a combination of powerful cosmological probes and tests will be necessary.

In this paper, we study how dark energy parameters are constrained from different combinations of cosmic microwave background (CMB) experiments, supernovae of type Ia (SNe Ia) data, and weak lensing surveys (WL) with and without tomography. In particular, we look for combinations of experiments that will be able to constrain these parameters well enough to settle decisively some of the dark energy questions, say to a few percent. When CMB measurements constrained the total energy density to $\Omega_T = 1.02 \pm 0.02$ to a one sigma level (Spergel et al. (2003); Bennet et al. (2003)), it became generally more accepted that spatial curvature is negligible. Thus, an uncertainty of a few percent on dark energy parameters could be set as a reasonable goal. Of course, one should bear in mind that it will remain always possible to construct dynamical dark energy models that are indistinguishable from a cosmological constant within these limits, and therefore, one needs to resort to cosmological tests beyond the equation of state measurements. A better scenario providing a decisive answer would be one in which one could show that dark energy is clearly not a cosmological constant.

It is certainly wise to probe the nature of dark energy using gradual steps. However, in both the scenarios mentioned above, one should keep in mind that the results and conclusions obtained from an analysis where the equation of state is assumed constant are subject to changes if the equation of state is allowed to vary with the redshift. In this paper, we consider dark energy with a varying equation of state.

We chose the combination CMB+SN Ia+WL as various studies have already shown that supernovae type Ia constitute a powerful probe of dark energy via distance-redshift measurements, see for example (Riess et al (1998); Garnavich *et al.* (1998); Filippenko & Riess (1998); Perlmutter, *et al.* (1999); Perlmutter S., *et al.* (1997); Riess et al (2000); Riess et al (2001)) (Tonry et al. (2003); Knop et al. (2003) ; Barris et al., (2004); Riess et al. (2004)). Also, several parameter forecast studies have shown that combining constraints from weak gravitational lensing with constraints from the CMB is a powerful combination to constrain dark energy; see, e.g. (Hu (2001); Huterer (2002); Huterer & Turner (2001); Benabed & Van Waerbeke (2003)) (Abazajian & Dodelson (2003); Refregier et al. (2003); Heavens (2003) ; Simon et al (2003); Jain & Taylor (2003)) (Bernstein & Jain (2004); Song & Knox (2004)). Importantly, weak lensing measurements are sensitive to both the effect of dark energy on the expansion history and its effect on the growth factor of large-scale structure. Furthermore, in addition to tightening the constraints, using independent probes will allow one to test the systematic errors of each probe, which are serious limiting factors in these studies. For each of these probes, much data will be available in the near and far future. For WL, there are many ongoing, planned and proposed surveys, such as the Deep Lens Survey (<http://dls.bell-labs.com/>) (Wittman et al.(2002)); the NOAO Deep Survey (<http://www.noao.edu/noao/noaodeep/>); the Canada-France-Hawaii Telescope (CFHT) Legacy Survey (<http://www.cfht.hawaii.edu/Science/CFHLS/>) (Mellier et al.(2001)); the Panoramic Survey Telescope and Rapid Response System (<http://pan-starrs.ifa.hawaii.edu/>); the Supernova Acceleration Probe (SNAP; <http://snap.lbl.gov/>) (Rhodes et al.(2003); Massey et al.(2003); Refregier et al.(2003)); and the Large Synoptic Survey Telescope (LSST; http://www.lsst.org/lsst_home.html) (Tyson (2002)). Similarly, there are many ongoing, planned and proposed SNe Ia surveys, such as the Supernova Legacy Survey (Pain et al. (2002); Pritchett (2004)) (SNLS); The Nearby Supernova Factory (SNfactory) (Wood-Vasey et al. (2004)); the ESSENCE project (Smith et al. (2002); Garnavich et al (2002); Kirshner et al. (2003)); Sloan Digital Sky Survey (SDSS) (Madgwick et al. (2003)); The Carnegie Supernova Project (Freedman et al. (2004)); and the Dark Energy Camera Project (DeCamera (2004)). We should mention that there are other noteworthy cosmological tools for probing dark energy that we did not consider in this study, notably clusters of galaxies (see for example (Mohr (2004); Wang et al.(2003)) and references therein), Lyman-alpha forests (see for example (Mandelbaum et al (2003); Seljak et al. (2004))), and baryonic oscillations (see for example (Eisenstein (2003); Seo & Eisenstein (2003); Blake & Glazebrook (2003); Linder (2003))).

For the CMB, we consider future constraints from 8 years of data from the Wilkinson Microwave Anisotropy Probe (WMAP-8) (Bennet et al. (2003); Spergel et al. (2003)), 1 year of data from the Planck satellite (PLANCK1), and 1 year of data from the Atacama Cosmology Telescope (ACT), see e.g. (Kosowsky (2003)). We use two sets of 2000 supernovae with $z_{max}=0.8$ and $z_{max}=1.5$ respectively, and consider two types of cosmic shear surveys: a ground-based like survey covering 70% of the sky with source galaxy redshift distribution having a median redshift $z_{med} \approx 1$, and a space-based like deep survey covering successively 1%, 10% and 70% of the sky with $z_{med} \approx 1.5$.

We take into account in our analysis systematic limits for the supernovae by adding a systematic uncertainty floor in quadrature following (Kim et al. (2003)). We also include for weak lensing the effect of the redshift bias and the shear calibration bias by adding and marginalizing over the corresponding parameters as in (Ishak et al. (2004)).

The constraints on the dark energy equation of state are parameterization dependent; see, e.g. (Wang & Tegmark (2004); Upadhye et al. (2004)). Also, there is a smearing effect due to double integration involved when using the equation of state (Maor et al. (2002); Maor et al. (2001)). In order to partly avoid this, one could probe directly the variations in the dark energy density using the data; see, e.g. (Wang & Mukherjee (2004); Wang & Freese (2004)). However, it has been argued that the equation of state is closer to the physics, as it also contains information on the pressure, and, trying to probe the equation

of state from the density leads to instability and bias (Linder (2004)). Therefore, we choose in this analysis to use both and parameterize the dark energy using its density $\rho_{de}(z)$ as well as two different parameterizations of its equation of state $w(z)$.

2 COSMOLOGICAL MODEL AND DARK ENERGY PARAMETERIZATION

2.1 Model

A total set of 13 parameters is considered as follows. For constraints from WL, we use: $\Omega_m h^2$, the physical matter density; Ω_Λ, w_0 and w_1 (or w_a), respectively the fraction of the critical density in a dark energy component and its equation of state parameters (see Sec. 2.2 (alternatively, we use the dark energy density parameters $\mathcal{E}_i \equiv \rho_{de}(z_i)/\rho_{de}(0)$ with $i = 1, 2$ (see section 2.2)); we use n_s ($k_0 = 0.05h/\text{Mpc}$) and α_s , the spectral index and running of the primordial scalar power spectrum at k_0 ; σ_8^{lin} , the amplitude of linear fluctuations. In order to parameterize some systematics, we include as a parameter z_p , the characteristic redshift of source galaxies (see Eq. 13), as well as ζ_s and ζ_r , the calibration parameters as defined in Ref. (Ishak et al. (2004)) which determine the absolute calibration error on the lensing power spectrum, (Hirata & Seljak (2003)), and the relative calibration between tomography bins (see Sec. 3.4). When we combine this with the CMB, we include $\Omega_b h^2$, the physical baryon density; τ , the optical depth to reionization; T/S the scalar-tensor fluctuation ratio. We assume a spatially flat Universe with $\Omega_m + \Omega_\Lambda = 1$. This fixes Ω_m and H_0 as functions of the basic parameters. We do not include massive neutrinos, or primordial isocurvature perturbations. For the supernova analysis, we use Ω_Λ, w_0, w_1 , (or $\mathcal{E}_1, \mathcal{E}_2$) and treat the magnitude parameter \mathcal{M} as a nuisance parameter. We use the fiducial model (e.g. Ref. (Spergel et al. (2003))) and add w_0 and w_1 : $\Omega_b h^2 = 0.0224$, $\Omega_m h^2 = 0.135$, $\Omega_\Lambda = 0.73$, $w_0 = -1.0$, $w_1 = 0.0$, $n_s = 0.93$, $\alpha_s = -0.031$, $\sigma_8 = 0.84$, $\tau = 0.17$, $T/S = 0.2$, $z_p = 0.76, 1.12$, $\zeta_s = 0.0$, and $\zeta_r = 0.0$.

2.2 Dark energy parameterization

As mentioned earlier, constraining the dark energy using its equation of state is known to be parameterization dependent, e.g. (Wang & Tegmark (2004); Upadhye et al. (2004)), and also suffers from a smearing due to the double integration involved (Maor et al. (2002); Maor et al. (2001)). Alternatively, one can probe directly the variations of the dark energy density as a function of redshift $\rho_{de}(z)$. On the other hand, it has been argued that the equation of state contains information on both the density and pressure of the dark energy and using the density to probe the equation of state may lead to instability and bias (Linder (2004)). We chose to study the constraints on dark energy using both approaches.

2.2.1 The equation of state

There are several parameterizations of the dark energy equation of state that have been used to study currently available data or to do parameter constraint projections. Discussions of the advantages and drawbacks of some of these parameterizations can be found in (Wang & Tegmark (2004); Upadhye et al. (2004)). We used here the following two parameterizations, which have no divergence at very large redshift:

$$\text{a) } (w_0, w_1)$$

Here w_1 represents the redshift derivative of $w(z)$ in the recent past as follows (see, e.g. (Upadhye et al. (2004)))

$$w(z) = \begin{cases} w_0 + w_1 z & \text{if } z < 1 \\ w_0 + w_1 & \text{if } z \geq 1. \end{cases} \quad (1)$$

The evolution of dark energy density with redshift is given by $\rho_{de}(z) = \rho_{de}(0)\mathcal{E}(z)$ where

$$\mathcal{E}(z) \equiv \begin{cases} (1+z)^{3(1+w_0-w_1)} e^{3w_1 z} & \text{if } z < 1, \\ (1+z)^{3(1+w_0+w_1)} e^{3w_1(1-2\ln 2)} & \text{if } z \geq 1. \end{cases} \quad (2)$$

$$\text{b) } (w_0, w_a)$$

Here the equation of state is parameterized as (Chevalier et al. (2001); Linder (2003))

$$w(a) = w_0 + w_a \frac{z}{1+z} = w_0 + w_a(1-a) \quad (3)$$

where a is the scale factor. The dark energy density evolves with $\mathcal{E}(a)$ now given by

$$\mathcal{E}(a) = a^{-3(1+w_0+w_a)} e^{-3w_a(1-a)}. \quad (4)$$

Table 1. CMB experiment specifications for Planck and ACT. The parameters used for WMAP 8 years are based on the projection of the one year operation and are described in section 5.

	f_{sky}	l_{max}	f(GHz)	θ_b (arcmin)	$\frac{\Delta T}{T}(10^{-6})$	$\frac{\Delta P}{T}(10^{-6})$
Planck-1	0.8	2500	100	9.5	2.5	4.0
			143	7.1	2.2	4.2
			217	5.0	4.8	9.8
	f_{sky}	l_{max}	f(GHz)	θ_b (arcmin)	$w_{\text{eff.}}(\text{sr}^{-1})$	
ACT-1	0.005	8000	150	1.7	3×10^{18}	

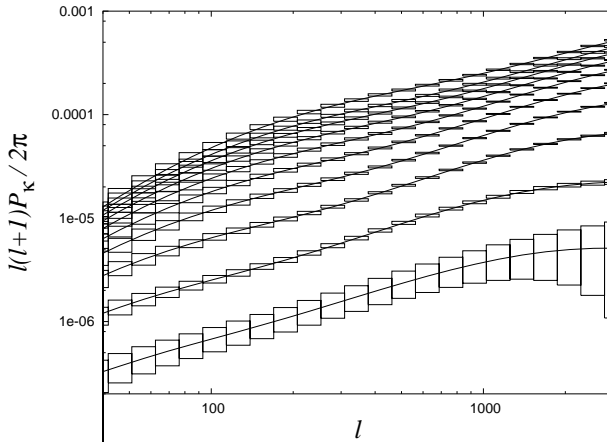


Figure 1. Convergence auto power spectra for the 10 tomography bins. All the parameters are fixed at their fiducial values. From the bottom to the top, the curves correspond to the redshift intervals $[0.0, 0.3], \dots, [2.7, 3.0]$. For each curve, we display the sample variance errors averaged over bands in l .

2.2.2 The density parameters: $\mathcal{E}_1 \equiv \frac{\rho_{de}(z_1)}{\rho_{de}(0)}$, $\mathcal{E}_2 \equiv \frac{\rho_{de}(z_2)}{\rho_{de}(0)}$

Following (Wang & Mukherjee (2004); Wang & Freese (2004)), we parameterize $\mathcal{E}(z) \equiv \frac{\rho_{de}(z)}{\rho_{de}(0)}$ as a continuous function interpolated between today and its amplitude parameters \mathcal{E}_1 and \mathcal{E}_2 corresponding respectively to $z=0.5$ and 1.0 , and remaining constant at higher redshifts. We use a polynomial interpolation as in (Wang & Mukherjee (2004); Wang & Freese (2004)) so

$$\mathcal{E}(z) = 1 + (4\mathcal{E}_1 - \mathcal{E}_2 - 3) \frac{z}{z_{max}} + 2(\mathcal{E}_2 - 2\mathcal{E}_1 + 1) \frac{z^2}{z_{max}^2}. \quad (5)$$

where the parameters \mathcal{E}_1 , and \mathcal{E}_2 will be constrained from the data. As suggested in (Wang & Mukherjee (2004)) and (Wang & Freese (2004)), we could use more density parameters than two as much more data will be available in the future, but we chose to use only two parameters in order to keep the number of parameters equal to the equation of state case and be able to make a fair comparison of the results. Departures of the density parameters from unity will be an indication of a redshift evolution of the dark energy density and will rule out a cosmological constant.

3 PROBING DARK ENERGY WITH COSMIC SHEAR

Weak lensing is a very promising tool for an era of precision cosmology. Already, several studies used currently available cosmic shear data to constrain various cosmological parameters (Contaldi et al.(2003); Van Waerbeke et al.(2002) et al.. (2002); Wang et al.(2003); Jarvis et al.(2003); Massey et al.(2004)). Using statistical inference theory, many other studies showed the promise of this probe (Hu & Tegmark (1999); Hu (2001); Huterer (2002); Abazajian & Dodelson (2003)) (Benabed & Van Waerbeke (2003); Takada & Jain (2004); Takada & White (2003); Heavens (2003) ; Jain & Taylor (2003)) (Bernstein & Jain (2004); Ishak et al. (2004); Simon et al (2003)). In particular, weak lensing was shown to constrain significantly the dark energy parameters. The advantage of weak lensing is that it is sensitive to the effect of dark energy on the expansion history and its effect on the growth factor of large-scale structure. Another advantage of weak lensing is that it allows one to construct new tests or techniques to probe cosmology. These include redshift bin tomography (Hu (1999); Hu (2002)), cross-correlation cosmography (Bernstein & Jain (2004)), and the use of higher order statistics such as the bis-

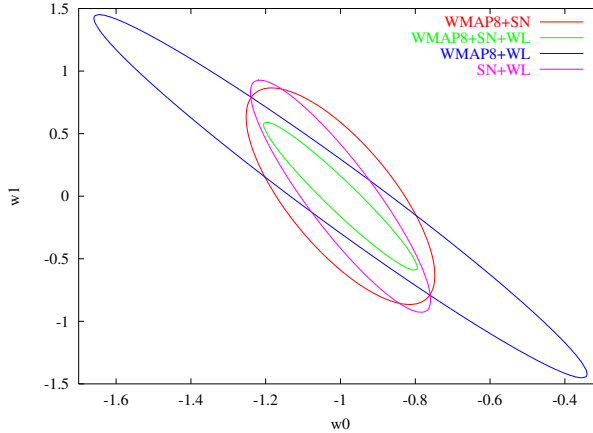


Figure 2. The 1σ confidence two-dimensional regions ($\Delta\chi^2 = 1$) for the (w_0, w_1) parameters. The plots contrast the constraints obtained from different combinations of 8 years of data from WMAP, 2000 SNe Ia with $z_{max} = 0.8$, and a ground-based like WL reference survey with $f_{sky} = 0.7$, $\bar{n} = 30$ gal/arcmin 2 , $\langle\gamma_{int}^2\rangle^{1/2} \approx 0.4$, and a median redshift $z_{med} \approx 1$.

pectrum; see, e.g. (Takada & Jain (2004)). We explore in this analysis the constraints obtained from the convergence power spectrum and multiple bin tomography.

3.1 Convergence power spectrum

Light rays traveling to us from background galaxies get deflected by mass fluctuations in large scale structures. This results in distortions of the sizes and shapes of these galaxies that can be described by the transformation matrix

$$A_{ij} \equiv \frac{\partial \theta_s^i}{\partial \theta_j} = \begin{pmatrix} 1 - \kappa - \gamma_1 & \gamma_2 \\ \gamma_2 & 1 - \kappa + \gamma_1 \end{pmatrix} \quad (6)$$

where θ_s is the angular position in the source plane; θ is the angular position in the image plane; κ is the convergence and describes the magnification of the size of the image; γ_1 and γ_2 are the components of the complex shear and describe the distortion of the shape of the image. In the weak gravitational lensing limit, $|\kappa|, |\gamma| \ll 1$.

The convergence is given by a weighted projection of the matter energy density fluctuations $\delta \equiv \delta\rho/\rho$ along the line of sight between the source and the observer,

$$\kappa(\hat{\theta}) = \int_0^{\chi_H} W(\chi) \delta(\chi, \chi\hat{\theta}) d\chi \quad (7)$$

where χ is the radial comoving coordinate and χ_H is the comoving coordinate at the horizon.

The convergence scalar field can be decomposed into multipole moments of the spherical harmonics as

$$\kappa(\hat{\theta}) = \sum_{lm} \kappa_{lm} Y_l^m(\hat{\theta}), \quad (8)$$

where

$$\kappa_{lm} = \int d\hat{\theta} \kappa(\hat{\theta}, \chi) Y_l^{m*}(\hat{\theta}). \quad (9)$$

The convergence power spectrum P_l^κ is then defined by

$$\langle \kappa_{lm} \kappa_{l'm'} \rangle = \delta_{ll'} \delta_{mm'} P_l^\kappa \quad (10)$$

and we will use it as our weak lensing statistic. In the Limber approximation, it is given by (Kaiser (1992); Jain & Seljak (1997); Kaiser (1998)):

$$P_l^\kappa = \frac{9}{4} H_0^4 \Omega_m^2 \int_0^{\chi_H} \frac{g^2(\chi)}{a^2(\chi)} P_{3D} \left(\frac{l}{\sin_K(\chi)}, \chi \right) d\chi. \quad (11)$$

where P_{3D} is the 3D nonlinear power spectrum of the matter density fluctuation, δ ; $a(\chi)$ is the scale factor; and $\sin_K \chi = K^{-1/2} \sin(K^{1/2} \chi)$ is the comoving angular diameter distance to χ (for the spatially flat universe used in this analysis, this reduces to χ). The weighting function $g(\chi)$ is the source-averaged distance ratio given by

$$g(\chi) = \int_\chi^{\chi_H} n(\chi') \frac{\sin(\chi' - \chi)}{\sin_K(\chi')} d\chi', \quad (12)$$

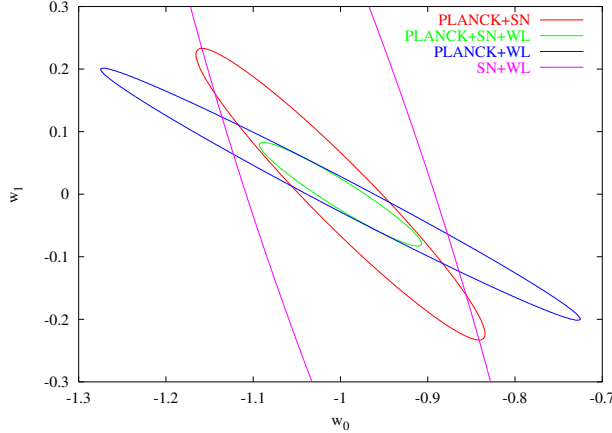


Figure 3. The 1σ confidence two-dimensional regions ($\Delta\chi^2 = 1$) for the (w_0, w_1) parameters. The plots contrast the constraints obtained from different combinations of 1 year of data from Planck, 2000 SNe Ia with $z_{max} = 0.8$, and a ground-based like WL reference survey with $f_{sky} = 0.7$, $\bar{n} = 30 \text{ gal/arcmin}^2$, $\langle\gamma_{int}^2\rangle^{1/2} \approx 0.4$, and a median redshift $z_{med} \approx 1$.

where $n(\chi(z))$ is the source redshift distribution normalized by $\int dz n(z) = 1$. For $n(z)$, we use the distribution (Wittman et al.(2000)):

$$n(z) = \frac{z^2}{2z_0^3} e^{-z/z_0}, \quad (13)$$

which peaks at $z_p = 2z_0$. For cosmic shear calculations, we integrate numerically the growth factor using (Linder & Jenkins (2003))

$$G'' + \left[\frac{7}{2} - \frac{3}{2} \frac{w(a)}{1+X(a)} \right] \frac{G'}{a} + \frac{3}{2} \frac{1-w(a)}{1+X(a)} \frac{G}{a^2} = 0 \quad (14)$$

where $G = D/a$ is the normalized growth factor with $D = \delta(a)/\delta(a_i)$,

$$X(a) = \frac{\Omega_m}{(1-\Omega_m)a^3\mathcal{E}(a)}, \quad (15)$$

and $\mathcal{E}(a)$ is as given in Eq. 4. We use the mapping procedure HALOFIT (Smith et a. (2003)) to calculate the non-linear power spectrum. We show in Fig. 1 convergence power spectra for the 10 tomographic bins. We also show the sample variance errors averaged over bands in l .

3.2 Weak lensing tomography

The separation of source galaxies into tomographic bins improves significantly the constraints on cosmological parameters, and particularly those of dark energy because tomography probes the growth of structure. The constraints obtained within different redshift bins are complementary and add up to reduce the final uncertainties. We explore here three tomography studies using two different types of cosmic shear surveys. For the first survey (ground-based like), the source galaxy redshift distribution has a median redshift $z_{median} = 1.0$, and we assume that the photometric redshift knowledge will allow one to split the source galaxies into successively 2 and 5 bins. For the second survey (space-based like), the source galaxy redshift distribution has a median redshift $z_{median} = 1.5$, and we assume a good knowledge of photometric redshifts and split the sources into 10 tomographic bins. For each redshift bin i , the weighting function is given by

$$g_i(\chi) = \begin{cases} \int_{\chi_i}^{\chi_{i+1}} d\chi' n_i(\chi') \frac{\chi' - \chi}{\chi'}, & \chi \leq \chi_{i+1} \\ 0, & \chi > \chi_{i+1} \end{cases} \quad (16)$$

where $n_i(\chi)$ is the bin normalized redshift distribution. The average number density of galaxies in this bin is $\Phi_i \bar{n}$ with the fraction Φ_i given by

$$\Phi_i = \int_{\chi_i}^{\chi_{i+1}} d\chi' n(\chi'). \quad (17)$$

For example, in the 2 bin case, the normalized distributions are given by

$$n^A(z) = \begin{cases} \frac{n(z)}{1-5/e^2} & z_p \leq 2z_0, \\ 0, & z_p > 2z_0, \end{cases} \quad (18)$$

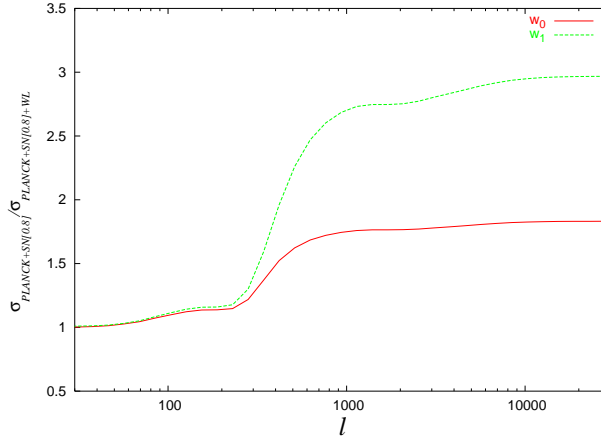


Figure 4. The improvement of the constraints as a function of the scales probed by the ground-based like weak lensing survey (no-tomography). The combination PLANCK1+SN[0.8]+WL is used here. The curves represent $\sigma_{PLANCK+SN[0.8]}/\sigma_{PLANCK1+SN[0.8]+WL}$ for w_0 and w_1 . The improvement from WL arises from probing non-linear scales ($l \gtrsim 100$), with a significant jump in the improvement between $l \sim 200$ and ~ 2000 for the reference survey considered.

and

$$n^B(z) = \begin{cases} 0, & z_p \leq 2z_0, \\ \frac{n(z)}{5/e^2}, & z_p > 2z_0. \end{cases} \quad (19)$$

For the 5 bins, we use redshift intervals of $\Delta z = 0.6$ over the redshift range $0.0 < z < 3.0$, and for the 10 bins we use intervals of $\Delta z = 0.3$. The convergence power spectra for the 10 bins with the respective sample variance errors averaged over bands in ℓ are shown in figure 1.

3.3 Fisher matrices for weak lensing

If the convergence field is Gaussian, and the noise is a combination of Gaussian shape and instrument noise with no intrinsic correlations, the Fisher matrix is given by:

$$F_{\alpha\beta} = \sum_{\ell=\ell_{\min}}^{\ell_{\max}} \frac{1}{(\Delta P_\kappa)^2} \frac{\partial P_\kappa}{\partial p^\alpha} \frac{\partial P_\kappa}{\partial p^\beta}; \quad (20)$$

where the uncertainty in the observed weak lensing spectrum is given by: (Kaiser (1992); Kaiser (1998))

$$\Delta P_\kappa(\ell) = \sqrt{\frac{2}{(2\ell+1)f_{sky}}} \left(P_\kappa(\ell) + \frac{\langle \gamma_{int}^2 \rangle}{\bar{n}} \right), \quad (21)$$

where $f_{sky} = \Theta^2 \pi / 129600$ is the fraction of the sky covered by a survey of dimension Θ in degrees, and $\langle \gamma_{int}^2 \rangle^{1/2}$ is the intrinsic ellipticity of galaxies. Guided by previous studies and taking into consideration the major difficulty of constraining both w_0 and w_1 , we considered an almost full sky ground-based like survey with $f_{sky} = 0.7$, a median redshift of roughly 1, an average galaxy number density of $\bar{n} = 30$ gal/arcmin², and $\langle \gamma_{int}^2 \rangle^{1/2} = 0.4$. We also model an ambitious space-based like survey with $f_{sky} = 0.01, 0.10$, and 0.70 , a median redshift of roughly 1.5, $\bar{n} = 100$ gal/arcmin², and $\langle \gamma_{int}^2 \rangle^{1/2} \approx 0.25$. We have used $\ell_{\max} = 3000$ since on smaller scales, the assumption of a Gaussian shear field underlying Eq. (20) and the HALOFIT approximation to the nonlinear power spectrum may not be valid for larger ℓ 's. For the minimum ℓ , we take the fundamental mode approximation:

$$\ell_{\min} \approx \frac{360 \text{ deg}}{\Theta} = \sqrt{\frac{\pi}{f_{sky}}}, \quad (22)$$

i.e. we consider only lensing modes for which at least one wavelength can fit inside the survey area. For tomography, the Fisher matrix is generalized using

$$F_{\alpha\beta} = \sum_{\ell_{\min}}^{\ell_{\max}} (\ell + 1/2) f_{sky} \text{Tr} \left(\mathbf{C}_\ell^{-1} \frac{\partial \mathbf{P}_\ell}{\partial p^\alpha} \mathbf{C}_\ell^{-1} \frac{\partial \mathbf{P}_\ell}{\partial p^\beta} \right), \quad (23)$$

where \mathbf{C}_ℓ is the covariance matrix of the multipole moments of the observables $C_\ell^{\kappa\kappa'} = P_\ell^{\kappa\kappa'} + N_\ell^{\kappa\kappa'}$ with $N_\ell^{\kappa\kappa'} = \delta_{\kappa\kappa'} \langle \gamma_{int}^2 \rangle / \Phi_i \bar{n}$ the power spectrum of the noise in the measurement.

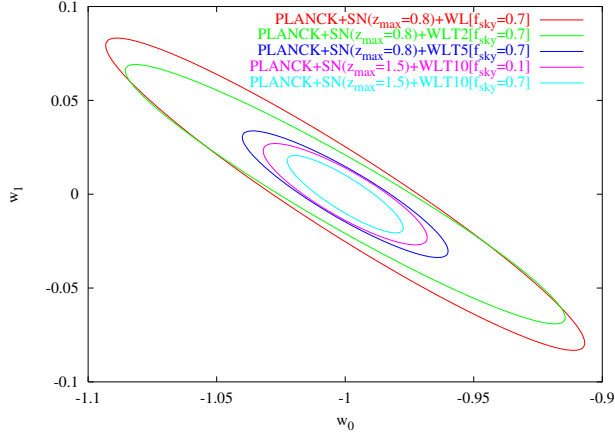


Figure 5. Tomography and the equation of state parameters: the 1σ confidence two-dimensional regions ($\Delta\chi^2 = 1$) for the parameters (w_0, w_1) . The plots contrast the constraints from different combinations of 1 year of data from Planck, 2000 uniformly distributed supernovae with $z_{max} = 0.8, 1.5$, the ground-based like lensing survey (WL), the ground-based like survey with successively 2 bin tomography (WLT2) and 5 bin tomography (WLT5), and the deep space-based like survey with 10 bin tomography (WLT10).

3.4 Weak lensing systematic effects

The probes considered here have systematic errors and nuisance factors that need to be well understood and well controlled in order for these constraints to be achievable. For cosmic shear, several systematic effects have been identified so far, see (Refregier (2003)) and references therein for an overview.

In this analysis, we included the effect of the shear calibration bias (Erben et al.(2001); Bacon et al. (2001)) (Hirata & Seljak (2003); Bernstein & Jarvis (2002); Kaiser (2000); Van Waerbeke & Mellier (2003)) on our results by marginalizing over its parameters. In this bias, the shear is systematically over or under-estimated by a multiplicative factor, and mimics an overall rescaling of the shear power spectrum. We used the absolute power calibration parameter ζ_s and the relative calibration parameter ζ_r between two redshift bins, following the parametrization used and discussed in (Ishak et al. (2004)). The calibration bias is not detected by the usual systematic tests such as the E and B modes decomposition of the shear field and the cross-correlation of the shear maps against the point-spread function (PSF) maps. In a weak lensing survey, ζ_s and ζ_r are parameters of the experiment that can in principle be determined by detailed simulations of the observations. We impose in this analysis a reasonable Gaussian prior of 0.04 on these parameters.

Another serious systematic is the incomplete knowledge of the source redshift distribution (Wittman et al.(2000)) (Ishak & Hirata (2005)) including the redshift bias and scattering. One can argue that as long as the scatter in the redshift ($\sigma(z) \approx 0.05$) is much smaller than the width of the redshift bin $\Delta z = 0.3$ (for our 10 bin tomography) the effect on the integrated results should be small. This is due to the fact that the scatter will only change slightly the shape of the edges of the window function that is used for the redshift integration within each bin. At the contrary, the redshift bias alters the overall distribution and has been known to affect significantly the cosmological parameter estimation (Refregier (2003); Ishak et al. (2004); Tereno et al. 2004). A remedy to this poor knowledge of the redshift distribution using spectroscopic redshift has been explored recently in (Ishak & Hirata (2005)). In the present analysis we marginalize over the redshift bias by including the characteristic redshift of the distribution as a systematic parameter z_s and we assume a reasonable Gaussian prior of 0.05 on this parameter.

It is important to question our assumption of gaussianity for the two weak lensing systematic errors that we considered here. So far, studies have made this assumption. The motivation for this assumption is the simplicity of the approximation but its justification needs to be addressed in dedicated lensing systematic studies. Thus our treatment of these two systematics is only valid under this assumption of gaussianity. For the redshift bias, one has to stress the requirement for a sufficiently large number of spectroscopic redshifts, see e.g. (Ishak & Hirata (2005)), and a sufficiently large number of source galaxies in order to reduce the uncertainties to a point where they can be approximated by Gaussians. Also, more narrow band colors and more accurate magnitudes (i.e. deeper exposure) are necessary in order to break degeneracies between the photometric redshifts. For the shear calibration bias, the errors cannot be made small enough by adding more data, and in this case simulations are necessary in order to estimate and address the non-gaussianity question. Massive sky image simulations on which the shear is measured and compared to the input will be necessary and such studies are planned to be carried out within ongoing projects in the lensing community, such as the Shear TEsting Programme (STEP) project (STEP collaboration (2005)). Indeed, studying the shear calibration bias using massive simulations is one of the goals of this project (STEP collaboration (2005)).

Hence, the reader should be aware that our treatment of shear calibration errors is valid only under the gaussianity assumption, and this needs to be checked by future simulation studies.

Finally, it is important to recall that there are systematic effects that were not included in this analysis (e.g. intrinsic alignments of galaxies, uncertainties associated with the non-linear mapping of the matter power spectrum, see (Refregier (2003)) and references therein for a list of other effects), however it is encouraging to note that many efforts are spent in order to study these and other lensing systematic effects and some progress has been made. With a better understanding of these limiting factors it will be possible to parameterize them and evaluate their effect on the cosmological parameter estimation.

4 PROBING DARK ENERGY WITH SUPERNOVAE TYPE IA

Supernovae of type Ia are powerful probes of dark energy, as when properly calibrated they become cosmological standard candles that can be used to measure distances as a function of redshift. The luminosity distance to a SN Ia is given by

$$d_L \equiv \sqrt{\frac{L}{4\pi F}} \quad (24)$$

where L is the intrinsic luminosity and F is the observed flux. The apparent magnitude of this SNa Ia can be written as

$$m = 5 \log_{10}(D_L) + \mathcal{M} \quad (25)$$

where $D_L \equiv H_0 d_L / c$ is the dimensionless luminosity distance, $\mathcal{M} \equiv M - 5 \log_{10}(H_0/c) + \text{constant}$ is the magnitude parameter, and M is the absolute magnitude, degenerate here with the Hubble parameter. In a spatially flat model

$$D_L(z) = (1+z) \int_0^z \frac{1}{\sqrt{(1-\Omega_\Lambda)(1+z')^3 + \Omega_\Lambda \mathcal{E}(z')}} dz', \quad (26)$$

where $\mathcal{E}(z)$ is as defined in Eq.(2). We use the Fisher matrix for the SNe Ia defined as (see, e.g. (Tegmark et al.(1998) ; Huterer & Turner (2001)))

$$F_{\alpha\beta} = \sum_{i=1}^N \frac{1}{\sigma_m(D_{L,i})^2} \frac{\partial D_{L,i}}{\partial p^\alpha} \frac{\partial D_{L,i}}{\partial p^\beta}. \quad (27)$$

We use two sets of 2000 SNe Ia uniformly distributed with $z_{max} = 0.8$ and $z_{max} = 1.5$. It is important to briefly note here that there are systematic uncertainties associated with supernova searches: these include luminosity evolution, gravitational lensing and dust; see, e.g. (SNAP (2003b)) and references therein. In order to partly include the effect of these systematics and the effect of the supernova peculiar velocity uncertainty (Tonry et al. (2003)), we follow (Kim et al. (2003); Upadhye et al. (2004)) and use the following expression for the effective magnitude uncertainty

$$\sigma_m^{eff} = \sqrt{\sigma_m^2 + \left(\frac{5\sigma_v}{\ln(10)cz}\right)^2 + N_{\{\text{per bin}\}} \delta_m^2} \quad (28)$$

where, a peculiar velocity of $\sigma_v = 500 \text{ km/sec}$ is assumed, and following (Kim et al. (2003); Upadhye et al. (2004)) we use $\delta_m = 0.02$ for space-based supernova survey data, and assume $\delta_m = 0.04$ for ground-based survey data. The quadrature relation (28) assures that there is an uncertainty floor set by the systematic limit δ_m so that the overall uncertainty per bin cannot be reduced to arbitrarily low values by adding more supernovae.

5 PROBING DARK ENERGY WITH CMB AND COSMIC COMPLEMENTARITY

CMB is a powerful cosmological probe; however, like other probes it suffers from some parameter degeneracies and needs to be combined with other data sets in order to provide tight constraints on dark energy parameters. For example, it is well known that cosmic shear and CMB have different types of degeneracies in their parameters, which are nicely broken when these probes are combined. Indeed, among the orthogonal directions of degeneracy between cosmic shear and CMB, are the known doublets (Ω_m, σ_8) , (h, n_s) , and (n_s, α_s) ; see, e.g. (Tereno et al. 2004). We use this cosmic complementarity in the present analysis where the statistical error (with some systematics included) on a given parameter p^α is given by:

$$\sigma^2(p^\alpha) \approx [(\mathbf{F}_{CMB} + \mathbf{F}_{WL} + \mathbf{F}_{SNe} + \Pi)^{-1}]^{\alpha\alpha}, \quad (29)$$

where Π is the prior curvature matrix, and \mathbf{F}_{CMB} , \mathbf{F}_{WL} and \mathbf{F}_{SNe} are the Fisher matrices from CMB, weak lensing, and supernovae, respectively. We only impose priors on the characteristic redshift and the calibration parameters by taking priors of $\sigma(z_p) = 0.05$ and $\sigma(\zeta_s) = \sigma(\zeta_r) = 0.04$ on the calibration parameters (corresponding to 2% rms uncertainty on the amplitude calibration; (Hirata & Seljak (2003))). We may add the CMB and weak lensing (WL) Fisher matrices together because the primary CMB anisotropies are generated at much larger comoving distance than the density fluctuations that

Table 2. Summary of the parameter (w_0, w_1) estimation errors (1σ uncertainties) from different combinations of probes. CMB experiments are WMAP 8 years, Planck 1 year, and ACT 1 year (unlensed spectra) combined with WMAP 8 years. (We did not include constraints from the Sunayev-Zeldovich effect or lensing of the CMB that ACT and PLANCK will be useful with.) The 2000 supernovae are uniformly distributed with $z_{max} = 0.8$. WL is for a ground-based like weak lensing survey with $f_{sky} = 0.7$, $\bar{n} = 30 \text{ gal/arcmin}^2$, $\langle \gamma_{int}^2 \rangle^{1/2} \approx 0.4$, and a median redshift $z_{med} \approx 1$. WLT2 refers to the same weak lensing survey but with 2 bin tomography. The best constraints from the combinations in this table are from PLANCK1+SN[0.8]+WLT2.

	CMB	+SN	+WL	+WLT2	+SN+WL	+SN+WLT2	SN+WL no-CMB	SN+WLT2 no-CMB
WMAP-8 alone								
$\sigma(w_0)$	3.73	0.25	0.66	0.35	0.21	0.11	0.24	0.11
$\sigma(w_1)$	5.65	0.87	1.45	0.66	0.59	0.26	0.93	0.35
WMAP8+ACT								
$\sigma(w_0)$	0.82	0.20	0.58	0.22	0.18	0.11	”	”
$\sigma(w_1)$	1.87	0.59	1.40	0.42	0.48	0.25	”	”
PLANCK-1 alone								
$\sigma(w_0)$	0.50	0.17	0.28	0.23	0.093	0.086	”	”
$\sigma(w_1)$	0.31	0.23	0.20	0.18	0.083	0.069	”	”

give rise to weak lensing, hence it is a good approximation to take them to be independent. For CMB, we project constraints from 8 years of WMAP data (WMAP-8), 1 year of PLANCK data (PLANCK-1), and 1 year of ACT data combined with WMAP-8. The experiment specifications used for Planck and ACT are listed in table (1). For 8 year WMAP, we include TT , TE , and EE power spectra, assuming $f_{sky} = 0.768$ (the Kp0 mask of Ref. (Bennet et al. (2003))), temperature noise of 400, 480, and $580 \mu\text{K}$ arcmin in Q, V, and W bands respectively (the rms noise was multiplied by $\sqrt{2}$ for polarization), and the beam transfer functions of Ref. (Page et al. (2003)).

6 RESULTS AND DISCUSSION

We calculated future constraints on dynamical dark energy parameters obtained from several combinations of cosmic microwave background experiments (CMB), supernova searches (SNe Ia), and weak lensing surveys (WL) with and without tomography. For CMB, we considered future constraints from 8 years of data from WMAP (WMAP8), one year of data from Planck (PLANCK1), and one year of data from the Atacama Cosmology Telescope (ACT1). We used two sets of 2000 supernovae with $z_{max} = 0.8$ (SN[0.8]) and $z_{max} = 1.5$ (SN[1.5]) respectively, and considered various cosmic shear reference surveys: an almost full sky (70%) ground-based like survey (WL) with successively 2 (WLT2) and 5 (WLT5) tomographic bins; a deep space-based like survey with 10 tomographic bins (WLT10) covering successively 1%, 10% and 70% of the sky. We combined these experiments in doublets and triplets, taking into account space-based or ground-based like experiments for supernovae and weak lensing. One should take the uncertainties obtained on the dark energy parameters from CMB-only Fisher matrices with some caution as some of them are large and the Fisher matrix approximation may not be valid. We compared our CMB-only constraints for Planck with those of reference (Hu (2001)) and found them in good agreement. For example, when we fix the parameters w_1 to compare with reference (Hu (2001)), we find that our $\{\sigma(\Omega_\Lambda) = 0.087, \sigma(w) = 0.31\}$ are in good agreement with $\{\sigma(\Omega_\Lambda) = 0.098, \sigma(w) = 0.32\}$ from (Hu (2001)). Importantly, the constraints we obtain from any combination of the three probes are significantly smaller than CMB-only and therefore the constraints obtained are good estimates of the low bound of the uncertainties. Our results are summarized in tables 2, 3, and 4 and in figures 2, 3, 4, and 5. We looked for combinations of experiments that will provide constraints that are small enough to answer conclusively some of the dark energy questions.

The first question that one would like to answer is whether dark energy is a cosmological constant or a dynamical component. The most decisive answer will be to rule out significantly the cosmological constant. A less decisive but very suggestive answer will be to show that dark energy parameters are those of a cosmological constant with a few percent uncertainty only. This can be compared to the case of spatial curvature in the universe: when CMB results constrained the total energy density to $\Omega_T = 1.02 \pm 0.02$ at the one sigma level, then it became generally more accepted that spatial curvature is negligible. However, it is important to note that it will remain always possible to build dark energy models that could have a set of parameters indistinguishable from those of a cosmological constant within the limits set. So in this scenario other types of tests than the equation of state will be required in order to close the question.

As shown in table 4, the combinations PLANCK1+SN[1.5]+WLT10 [$f_{sky} = 0.1$] and PLANCK1+SN[0.8]+WLT5 [$f_{sky} = 0.7$] provide impressive constraints that reach the goal set. This is followed by the constraints from PLANCK1+SN[1.5]+WLT10 [$f_{sky} = 0.01$]. One should note here that for the equation of state parameters, only small additional improvements to

Table 3. Same as table 2 but for the dark energy parameterization (w_0, w_a) . As usual the errors on w_a are larger than those on w_1 (roughly equal to twice the errors on w_1). The best constraints in this table are from PLANCK1+SN[0.8]+WLT2.

	CMB	+SN	+WL	+WLT2	+SN+WL	+SN+WLT2	SN+WL no-CMB	SN+WLT2 no-CMB
WMAP-8 alone								
$\sigma(w_0)$	1.84	0.24	0.46	0.39	0.21	0.14	0.26	0.14
$\sigma(w_a)$	3.03	1.25	1.61	1.24	0.92	0.53	1.37	0.76
ACT+WMAP8								
$\sigma(w_0)$	0.52	0.21	0.27	0.42	0.19	0.14	”	”
$\sigma(w_a)$	1.83	0.92	0.85	1.48	0.76	0.50	”	”
PLANCK-1 alone								
$\sigma(w_0)$	0.67	0.15	0.28	0.24	0.097	0.088	”	”
$\sigma(w_a)$	0.52	0.30	0.32	0.29	0.133	0.111	”	”

these constraints are obtained when an extremely ambitious sky coverage of 70% is considered for PLANCK1+SN[1.5]+WLT10 [$f_{sky} = 0.7$]. Finally, the constraints on the equation of state parameters from PLANCK1+SN[0.8]+WLT2 [$f_{sky} = 0.7$] are not small enough for the criterion of a few percent set above.

Another test to answer the same question above is by probing directly the dark energy density at various redshift points. For example, if future data will show significant departures of the parameters \mathcal{E}_1 or \mathcal{E}_2 (see Sec. 2.2), from unity then a cosmological constant can be ruled out conclusively. Our analysis shows that this might be a less difficult test as even PLANCK+SN[0.8]+WLT5 [$f_{sky} = 0.7$] has the potential to achieve $\sigma(\mathcal{E}_1) = 0.012$ and $\sigma(\mathcal{E}_2) = 0.049$.

A second question of interest is what combination of experiments could distinguish between some currently proposed models of dark energy. Of particular interest are models that predict an equation of state with parameters that are significantly different from those of a cosmological constant. For example, one could consider quintessence tracker models (Zlatev et al.(1999)) or super-gravity inspired models (Brax et al.(1999)), for which, $w_0 \gtrsim -0.8$ and $dw/dz(z = 0) \sim 0.3$. From our tables, we see that the distinction between these models and a cosmological constant can be achieved by several different combinations of experiments with different levels of precision.

Our tables 2 and 3 show that after combining Planck and supernova constraints, weak lensing without tomography adds an improvement of roughly a factor of 2 or better to the constraints. As shown in figure 4, the WL-improvement arises from probing non-linear scales ($l \gtrsim 100$), with a significant jump between $l \sim 200$ and ~ 2000 for the ground-based like survey considered. Adding 2 bins tomography to the lensing survey provides an additional factor of 2 improvement to the combination WMAP8+SN[0.8]+WL and to combination ACT1+WMAP8+SN[0.8]+WL. We mention here that these results do not include constraints from Sunayev-Zeldovich effect or lensing of the CMB, that ACT and PLANCK will be useful with.

In table 4 and figure 5 we summarize our results on multiple-bin tomography. The constraints on the equation of state parameters from PLANCK1+SN[1.5] improve by factors 3-5 when WLT10 with $f_{sky} = 0.1$ is added to the combination. Also, the constraints on the equation of state parameters from PLANCK1+SN[0.8]+WLT5 [$f_{sky} = 0.7$] are roughly factors of 3-6 better than those obtained from PLANCK1+SN[0.8]. Thus, we find that the improvements obtained from multiple-bin tomography lensing surveys are important for the questions raised at the beginning of this section as it brings the uncertainties significantly closer to the goal of a few percent. Therefore, the present study shows that tomography is very useful to add further improvements to the constraints on dark energy parameters using both ground-based experiments and space-based experiments. The precise discussion of the technical and instrumental feasibility of multiple-bin tomography from ground or from space is beyond the scope of this paper and should be addressed somewhere else.

We took care to include some systematic effects in our analysis. We parameterized the weak lensing calibration bias and assumed reasonable priors of 0.04 on the calibration parameters. We also parameterized the redshift bias and used a reasonable prior of 0.05. However, there are other systematic effects that we did not include and that may affect our results. For example, we did not include the effect of intrinsic correlations between the lensing source galaxies on our results (Croft & Metzler (2000); Heavens et al.(2000); Lee & Pen(2000); Catelan et al.(2001); Crittenden et al.(2001); Brown et al.(2002)) (Jing (2002); Jarvis et al.(2003); Heymans et al.(2004); Hirata & Seljak (2004)), and we used the HALOFIT fitting formula to evaluate the non-linear matter power spectrum (full simulations should be used for real data analysis). As discussed in section 3.4, our inclusion of these two lensing systematics assumed their gaussianity. The effect of these systematics on our results is thus valid only under this approximation. Future dedicated studies of weak lensing systematic effects should address the issue of non-gaussianity. Also, following previous work, we included in our supernova constraints a conservative systematic limit, but more studies need to be done there as well.

Nevertheless, our results show that after the combination of CMB, supernovae, and weak lensing surveys, tomography

Table 4. Various tomography analyses: a comparative summary of the constraints (1σ uncertainties) on the different dark energy parameterizations from Planck-1, 2000 uniformly distributed supernovae with $z_{max} = 0.8, 1.5$, the ground-based like lensing survey with successively 2 bin tomography (WLT2) and 5 bins (WLT5), and the deep space-based like survey with 10 bin tomography (WLT10). The results are presented for the dark energy parameters $\{w_0, w_1\}$, $\{w_0, w_a\}$ and $\{\mathcal{E}_1 \equiv \rho_{de}(z = 0.5)/\rho_{de}(0), \mathcal{E}_2 \equiv \rho_{de}(z = 1.0)/\rho_{de}(0)\}$

PLANCK-1 alone	+SN($z_{max} = 1.5$)	+SN($z_{max} = 0.8$) +WLT2 [$f_{sky} = 0.7$]	+SN(0.8)+WLT5 [$f_{sky} = 0.7$]	+SN(1.5)+WLT10 [$f_{sky} = 0.01$]	+SN(1.5)+WLT10 [$f_{sky} = 0.1$]	+SN(1.5)+WLT10 [$f_{sky} = 0.7$]
$\sigma(w_0)$	0.50	0.11	0.086	0.04	0.048	0.032
$\sigma(w_1)$	0.31	0.13	0.069	0.034	0.042	0.027
$\sigma(w_0)$	0.67	0.12	0.088	0.041	0.049	0.033
$\sigma(w_a)$	0.52	0.21	0.111	0.056	0.067	0.040
$\sigma(\mathcal{E}_1)$	0.11	0.048	0.029	0.012	0.013	0.010
$\sigma(\mathcal{E}_2)$	0.32	0.12	0.065	0.049	0.082	0.040

with very large fractions of the sky and many redshift bins has the potential to add key improvements to the dark energy parameter constraints by bringing them to the level of a few percent.

On the other hand, the requirement for very ambitious and sophisticated surveys in order to achieve some of these constraints, and the difficulty to obtain any further significant improvements, even with the most ambitious survey we considered, suggest the need for new tests to probe the nature of dark energy in addition to constraining its equation of state.

ACKNOWLEDGMENTS

The author thanks David Spergel for support and for useful discussions. The author thanks N. Bahcall, O. Doré, C. Hirata, P. Steinhardt, A. Upadhye, and L. Van Waerbeke for useful comments. The author acknowledges the support of the Natural Sciences and Engineering Research Council of Canada (NSERC) and the support of NASA Theory Award NNG04GK55G.

REFERENCES

Abazajian K., Dodelson S., 2003, Phys. Rev. Lett. 91 041301
 Bacon D.J., *et al.*, 2001, MNRAS, 325, 1065
 Barris B.J., *et al.*, 2004, ApJ, 602, 571
 Bennett C. L., *et al.*, 2003, ApJ Suppl., 148, 1
 Bennett C. L., *et al.*, 2003, ApJ Suppl., 148, 67
 Bernstein G. M., Jain B., 2004, ApJ, 600, 17
 Bernstein G. M., Jarvis M., 2002, AJ123, 583.
 Benabed K., Van Waerbeke L., 2003, astro-ph/0306033.
 Blake C., Glazebrook K., 2003, AJ, 594, 665
 Brax P., Martin J., 1999, Phys. Lett. B, 468, 40
 Brown M., *et al.* 2002, MNRAS, 333, 501.
 Catelan, *et al.*, 2001, MNRAS, 320, L7
 Carroll S. M., *et al.*, 1992, ARAA, 30, 499
 Chevalier M., *et al.*, 2001, Int. J. Mod. Phy. D , 10, 213
 Crittenden R. G., *et al.*, 2002, ApJ, 559, 552
 Crof R., Metzler C., 2000, ApJ, 545, 561
 Contaldi C. R., *et al.* (2003), Phys. Rev. Lett., 90, 221303
 DECam, see <http://home.fnal.gov/~annis/astrophys/deCam/>
 Eisenstein D.J., 2003, astro-ph/0301623
 Erben T. *et al.*, (2001), å, 366, 717
 Filippenko A.V., Riess A.G., 1998, Phys. Rept., 307, 31
 Freedman W. L., for the Carnegie Supernova Project. Conference Proceedings, NOAO Workshop, Tucson, March, 2004, "Observing Dark Energy", eds. S. Wolff & T. Lauer; astro-ph/0411176
 Garnavich P. M. *et al.*, 1998, ApJ, 509, 74
 Garnavich P. M., *et al.*, 2002, Bull. Am. Astron. Soc., 34, 1233
 Heavens A., 2003, MNRAS, 343, 1327
 Heavens A., *et al.*, 2000, MNRAS, 319, 649
 Heymans C., *et al.*, 2004, MNRAS, 347, 895
 Hirata C., Seljak U., 2003, MNRAS, 343, 459.
 Hirata C., Seljak U., 2004, Phys. Rev. D, 70, 063526
 Hoekstra H. 2004, MNRAS, 347, 1337
 Hu W., 1999, ApJ Lett., 522 L21
 Hu W., 2001, Phys. Rev. D 65, 023003

Hu W., 2002, Phys. Rev. D 66, 083515
 Huterer D. 2002, Phys. Rev. D 65, 063001
 Huterer D., Turner M. S., 2001, Phys. Rev. D, 64, 123527
 Hu W., Tegmark M., 1999, ApJ Lett., 514, L65
 Ishak M., 2005, astro-ph/0504416
 Ishak M., et al., 2004, Phys. Rev. D, 69, 083514
 Ishak M., Hirata C., 2005, Phys. Rev. D, 71, 023002
 Kim et al., 2003, MNRAS, 347 (2004) 909
 Jain B., Seljak U. 1997, ApJ, 484, 560
 Jain B. , Taylor A., 2003, Phys. Rev. Lett., 91, 141302
 Jarvis M, et al., 2002, AJ, 125, 1014
 Jing Y.P. 2002, MNRAS, 335, L89
 Kaiser N., 1998, ApJ, 498, 26
 Kaiser N. 1992, ApJ, 388, 272
 Kaiser N., 2000, ApJ, 537, 555
 Knop R. A., et al., 2003, ApJ, 598, 102
 R. P. Kirshner, et al., American Astronomical Society Meeting 202 (2003) [ADS bib. code 2003AAS..202.2308K] [see also <http://www.ctio.noao.edu/wsne>].
 Kosowsky A., et al. (2003), New Astron. Rev. 47, 939
 Lee J. , Pen U. 2000, ApJ Lett., 532, L5
 Linder E., 2003, Phys. Rev. Lett., 90, 091301
 Linder E., 2003, Phys. Rev. D., 68, 083504
 Linder E., 2004, astro-ph/0406189
 Linder E., Jenkins A., 2003, MNRAS, 346, 573
 Ma C-P, Caldwell R.R., Bode P., Wang L., 1999, ApJ Lett., 521, 1
 D. S. Madgwick, et al., 2003, ApJ, 599, L33
 Maor I., et al, 2002, Phys. Rev. D, 65, 123003
 Maor I., et al, 2001, Phys. Rev. Lett., 86, 6; Erratum-ibid., 87, 049901
 Mandelbaum et al., 2003, MNRAS, 344, 776.
 Massey R., et al., 2004, astro-ph/0404195
 Massey R., et al, 2003, astro-ph/0304418
 Mellier Y, 2001, Mining the Sky, pp. 540–+.
 Mohr J.J., 2004, astro-ph/0408484
 Padmanabhan T., 2003, Phys. Rep., 380, 335
 R. Pain, et al., 2002, Bull. Am. Astron. Soc., 34, 1169
 Page L., et al., 2003, ApJ Suppl. Ser. **148**, 37
 Perlmutter S., et al., 1999, ApJ, 517, 565
 Perlmutter S., et al., 1997, Bull. Am. Astron. Soc., 29, 1351
 Pritchett C. J., 2004, astro-ph/0406242
 Refregier A., 2003, ARAA, 41, 645
 Refregier A. et al., 2003, astro-ph/0304419
 Refregier A., et al. 2003, astro-ph/0304419
 Riess A. G., et al., 1998, AJ, 116, 1009
 Riess A. G., et al., 2000, ApJ, 536, 62
 Riess A. G., et al., 2001, ApJ, 560, 49
 A. G. Riess, et al., 2004, ApJ, 607, 665
 Rhodes J., et al., 2003, astro-ph/0304417.
 Sahni V., Starobinsky A., 2000, Int.J.Mod.Phys., D9, 373
 Seljak U., et al, 2004, astro-ph/0407372
 Seo H., Eisenstein D., 2003, AJ, 598, 720
 Simon P., King L. J., Schneider P., 2003, astro-ph/0309032
 Smith R. C., et al., 2002, Bull. Am. Astron. Soc., 34, 1232
 Smith R.E., et al. 2003, MNRAS, 341, 1311
 Aldering G., et al., 2004, astro-ph/0405232
 Song Y. S. , Knox L., (2004), astro-ph/0312175
 Spergel L., et al., 2003, ApJ Suppl., 148, 175
 STEP collaboration: see e.g. Heymans C., et al., for the STEP collaboration, 2005, preprint astro-ph/0506112; <http://www.physics.ubc.ca/~heymans/step.html>
 Takada M., White M. 2003, astro-ph/0311104
 Takada M., Jain B., 2004, MNRAS, 348, 897.
 Tereno, I, 2005, *à*, 429, 383
 Tegmark et al., 1998, astro-ph/9805117
 Tonry J.L., et al, 2003, ApJ, 594, 1
 Turner M.S., 2000, Phys. Rep., 333, 619
 Tyson J. A., in Survey and Other Telescope Technologies and Discoveries. Edited by Tyson, J. Anthony; Wolff, Sidney. Proceedings of the SPIE, Volume 4836, pp. 10-20 (2002).
 Upadhye A., Ishak M., Steinhardt P., 2004, astro-ph/0411803.
 Van Waerbeke L., et al 2002, A&A, 393, 369.

Van Waerbeke L., Mellier Y., 2003, astro-ph/0305089
Wang Y., Mukherjee P., 2004, ApJ, 606, 654
Wang Y. , Freese K. 2004, astro-ph/0402208
Wang Y. , Tegmark M., 2004, Phys.Rev.Lett., 92, 241302
Wang S. et al., 2004, Phys. Rev. D, 70, 123008
Wang X. et al., 2003, Phys. Rev. D, 68, 123001
Weinberg S., 1989, Rev. Mod. Phys., 61, 1
Wittman D. M. 2002, Survey and Other Telescope Technologies and Discoveries. Edited by Tyson, J. Anthony; Wolff, Sidney. Proceedings of the SPIE, Volume 4836, pp. 73-82.
Wood-Vasey W. M., *et al.*, 2004, New Astron. Rev. 48, 637
Wittman et al., 2000, Nature, 405, 143
Zlatev I, Wang L., , Steinhardt P.J., 1999, Phys. Rev. Lett. 82, 896